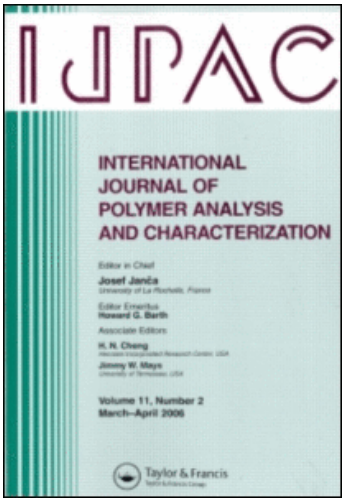

International Journal of Polymer Analysis and Characterization
Publication details, including instructions for authors and subscription information:
http://www.informaworld.com/smpp/title~content=t713646643

Predicting Mid-Infrared Spectra from Near-infrared Spectra

Raymond Lew[ab]; Anwer Khan[a]; Stephen T. Balke[a]
[a] Department of Chemical Engineering and Applied Chemistry, University of Toronto, Toronto, Ontario, Canada [b] DuPont Company, Experimental Station, Wilmington, DE

To cite this Article Lew, Raymond , Khan, Anwer and Balke, Stephen T.(1995) 'Predicting Mid-Infrared Spectra from Near-infrared Spectra', International Journal of Polymer Analysis and Characterization, 1: 3, 231 — 243
To link to this Article: DOI: 10.1080/10236669508233877
URL: http://dx.doi.org/10.1080/10236669508233877

Int. J. Polymer Analysis & Characterization
1995, Vol. 1, pp. 231–243
Reprints available directly from the publisher
Photocopying permitted by license only

Predicting Mid-Infrared Spectra from Near-infrared Spectra

RAYMOND LEW,[1] ANWER KHAN and STEPHEN T. BALKE*

Department of Chemical Engineering and Applied Chemistry, University of Toronto, Toronto, Ontario, Canada M5S 1A4

(Received Sept. 15, 1993)

Near-infrared (NIR) analysis is increasingly used in the food industry and, more recently, in chemistry monitoring of polymer processes. However, quantitative interpretation is often highly empirical and subject to some distrust by many spectroscopists. In contrast, mid-infrared (MIR) analysis is widely accepted and the spectra often readily interpreted. This work provides further information on a recent, unifying application of a multivariate method termed "partial least squares". A PLS model was generated given a series of NIR and MIR calibration spectra. This model was used to predict the MIR spectrum of an "unknown" polyethylene–polypropylene blend given its NIR spectrum obtained from in-line monitoring of the polymer melt and extruder.

KEY WORDS Near-infrared, polymer blend, mid-infrared, partial least squares, spectroscopy

INTRODUCTION

The primary reason why near-infrared spectroscopy (NIR) is sometimes preferred over mid-infrared (MIR) spectroscopy is that absorption is generally very weak in the NIR region; thus, path lengths need to be very long. As shown in Table I, typical path lengths in the NIR region are more than an order of magnitude longer than those used in the MIR region. Two specific examples of the consequences are (i) when NIR diffuse reflectance analysis is used, essentially no sample preparation is required (e.g., pellets directly from an extruder can be poured into a large quartz cell and scanned) and (ii) when transmission NIR with fiber optics are used to monitor composition in polymer melt flowing through an extruder, the distance between the end of the transmitting probe and that of the receiving probe in the melt is typically as large as 0.5 cm. (i.e., flow between the probe tips is readily maintained).

NIR analysis has been used for other reasons as well. As Table I shows, the response in the NIR region consists mainly of overtone and combination bands. Some species have much stronger absorption in this region than others: hydroxyl

[1]Present address: DuPont Company, Experimental Station, P.O. Box 80228, Wilmington, DE 19880-0228.

*Author to whom correspondence should be addressed.

TABLE I

Comparison of MIR and NIR

	MIR	NIR
Wavelength (nm)	2500-50000	800-2500
(cm^{-1})	4000-200	12500-4000
Vibrational Mode	Fundamental	Overtones & Combinations
Peaks	Narrow, Resolved	Broad, Overlapped
Typical Path Length	0.1 mm	0.5 cm

(O-H) and amine (N-H) groups are important examples. Much of the earlier NIR work centered on these groups because of their presence in agricultural and food products [1, 2].

There are two main reasons why NIR is not more widely employed: (i) just as some species have much stronger absorption in the region, some have such weak absorption relative to others that they cannot be discerned, and (ii) the overtone and combination bands are very broad and overlapped. The first reason limits applicability but tends to be very system dependent. Thus, the main response to this reason has been to empirically select acceptable systems. The second reason means that interferences amongst absorbances can readily spoil attempts to correlate absorbance-at-one-wavelength versus concentration correlations. Although such attempts are sometimes useful, a major impetus to the use of NIR has been the employment of a computer-implemented technique known as "partial least squares" (PLS).

Partial least squares, however, is a complex numerical method. Effective commercial software packages are now available, but the method is distrusted. For example, a typical application of the method might be to provide the concentration of a certain polymer or additive in a mixture. Inspection of this "single number" appearing from a "black box" computer program is obviously not very reassuring. Software suppliers emphasize the use of certain diagnostic plots in their software —standard error of prediction plots, loading plots, and score plots, for example. These are very useful and need to be precisely inspected. However, the idea underlying our work is that for complex materials, such as polymers, additional (reassuring) chemistry information is needed from application of PLS to the NIR spectrum.

Mid-infrared spectra are widely used in polymer science both qualitatively and quantitatively. However, NIR analysis increasingly is being used [3–6]. If the MIR spectrum corresponding to the obtained NIR spectrum could be calculated, an analyst could immediately see whether the NIR spectrum was reasonable. Furthermore, the whole MIR spectrum would be available for interpretation. Barton et al. [7] attempted to approach this problem by calculating and mapping correlation coefficients corresponding to the absorbances observed for MIR with those for NIR. However, considerable intercorrelation across the entire spectrum was observed! Recently, we have shown how it is possible to generate the MIR spectrum from the NIR spectrum using PLS [8]. This paper further explains this approach.

THEORY

Quantitative Analysis

In MIR analysis, often a single wavelength is selected and Beer's law used.

$$a = ck \tag{1}$$

Where a is absorbance, c concentration of the absorbing species, and k the extinction coefficient.If q different species are present and can all possibly absorb over the same wavelength range, then we can select n wavelengths and measure the absorbance at each of these wavelengths for all m of our samples. Thus, we now have $n \times m$ equations, one for each absorbance measurement. Written for two samples the equations are:

Sample 1

$$\begin{aligned} a_{11} &= c_{11}k_{11} + c_{12}k_{21} + \cdots + c_{1q}k_{q1} \\ a_{12} &= c_{11}k_{12} + c_{12}k_{22} + \cdots + c_{1q}k_{q2} \\ &\cdots\cdots\cdots\cdots\cdots\cdots\cdots \\ a_{1n} &= c_{11}k_{1n} + c_{12}k_{2n} + \cdots + c_{1q}k_{qn} \end{aligned} \tag{2}$$

Sample 2

$$\begin{aligned} a_{21} &= c_{21}k_{11} + c_{22}k_{21} + \cdots + c_{2q}k_{q1} \\ a_{22} &= c_{21}k_{12} + c_{22}k_{22} + \cdots + c_{2q}k_{q2} \\ &\cdots\cdots\cdots\cdots\cdots\cdots\cdots \\ a_{2n} &= c_{21}k_{1n} + c_{22}k_{2n} + \cdots + c_{2q}k_{qn} \end{aligned}$$

In matrix form, equations for all m samples can be written simply:

$$A = CK \tag{3}$$

where A is the $m \times n$ matrix of measured absorbances, C is the $m \times q$ matrix of species concentrations, and K is the $q \times n$ matrix of extinction coefficients.

The usual procedure involves solving these equations for the extinction coefficients K in a "calibration" step followed by use of the K values in a "prediction" step to obtain the concentration values for an unknown sample [9–14]. When MIR is used, the method employed is "classical least squares". The problem examined here is to generate an MIR spectrum from an NIR spectrum. Because of each wavelength, Beer's law is obeyed in both the NIR and MIR, we can write the

matrix equation describing each MIR measured absorbance with each and every measured NIR measured absorbance:

$$A_{\text{MIR}} = A_{\text{NIR}} K \tag{4}$$

where K is the matrix of regression coefficientsresulting from performing multiple linear regression on the MIR and NIR absorbance data.

However, if there are say, 10 samples and 140 wavelengths (1400 absorbance values for each of MIR and NIR), then the $140 \times 140K$ matrix represents 19,600 values! The many wavelengths where the MIR and NIR do not correlate, combined with the matrix sizes, defeat numerical solution attempts.

In PLS, the absorbance data for MIR and for NIR is expressed as the product of two matrices, similar in form to the Beer's law formulation of Equation (3) [11–20]. The matrices forming the product are, however, no longer concentrations and extinction coefficients. They are now "scores" ($T_{\text{MIR}}, T_{\text{NIR}}$) and "loadings" ($P_{\text{MIR}}, P_{\text{NIR}}$):

$$A_{\text{NIR}} = T_{\text{NIR}} P_{\text{NIR}}$$

$$A_{\text{MIR}} = T_{\text{MIR}} P_{\text{MIR}} \tag{5}$$

Where A is still the $m \times n$ matrix of absorbances but now T is a $m \times h$ matrix of scores and P is an $h \times n$ matrix of loadings. Equation (5) is used to model the absorbance data using PLS. The relationship between the NIR and MIR data is through T and is a result of regressing the matrices against one another. If h is 3, then there are three linear combinations of scores and loadings (three "factors") that will result in the observed absorbance.

$$\begin{aligned}
a_{11} &= t_{11} p_{11} + t_{12} p_{21} + t_{13} p_{31} \\
a_{12} &= t_{11} p_{12} + t_{12} p_{22} + t_{13} p_{32} \\
&\cdots\cdots\cdots\cdots\cdots\cdots \\
a_{21} &= t_{21} p_{11} + t_{22} p_{21} + t_{23} p_{31} \\
a_{22} &= t_{21} p_{12} + t_{22} p_{22} + t_{23} p_{32} \\
&\cdots\cdots\cdots\cdots\cdots\cdots \\
a_{mn} &= t_{m1} p_{11} + t_{m2} p_{21} + t_{m3} p_{3n}
\end{aligned} \tag{6}$$

Because of the lower dimensionality of the T and P matrices compared to the K matrix of Equation (4), this is now a solvable problem. The solution for 1400 absorbance values now involves 900 data values instead of the 19,600 with classical least squares.

The scores T are actually numerically transformed spectral absorbance values. Most of the dominant information is contained within the first factors of the score and loading P matrices. The factor loadings show the relative importance of the variables (wavelength) with respect to a factor.

The number of factors required to model the data is an important consideration. It requires calculation of the square error of prediction (SEP) for each factor added. The SEP in terms of the spectral absorbances is given as:

$$\mathrm{SEP}(F) = \frac{1}{N_\lambda}\sum_{j=1}^{N_\lambda}\left[\frac{1}{N_s}\sum_{j=1}^{N_s}\left(A(i,j) - A_{F,\mathrm{Pred}}(i,j)\right)^2\right] \quad (7)$$

SEP = standard error of prediction

F = factor number

N_λ = total number of wavelengths

N_s = total number of samples (or spectra)

A = measured absorbance

$A_{F,\mathrm{Pred}}$ = predicted model absorbance for factor, F

i = sample number

j = wavelength number

In applying PLS, the above mentioned quantities are displayed graphically as spectra, standard error of prediction plots, and score plots in order to assess the modeling. Examples of these plots are shown in the Results and Discussion section.

Finally, once the data is modeled—i.e., the loading and score matrices are obtained from a calibration set, and the optimum number of factors is decided upon—these matrices can be used with an unknown NIR spectrum to transform that spectrum into a MIR spectrum (or vice versa, if desired).

EXPERIMENTAL

Extrusion: Polypropylene (PP6631, Himont Canada, Montreal, Quebec) and high-density polyethylene (HDPE 4052N, Dow Chemical Canada, Sarnia, Ontario) blends were produced by melt mixing of the two homopolymers in an extruder. A Deltaplast D40-150-24 single-screw extruder was used for processing operating at 200°C and 40 rpm. The extrudate strands from the extruder were run through a cooling bath and pelletized using a Model 881251 Laboratory Pelletizer (Brabender Instruments, New Jersey).

In-Line NIR Monitoring: In-line monitoring was accomplished using a Guided Wave (California) Model 260 NIR optic spectrophotometer. The Model 260 is a post-dispersive scanning spectrophotometer equipped with a lead sulfide detector. A tungsten-halogen lamp is used as a source with light dispersion accomplished using a concave holographic grating with 300 lines/mm. Figure 1 shows the

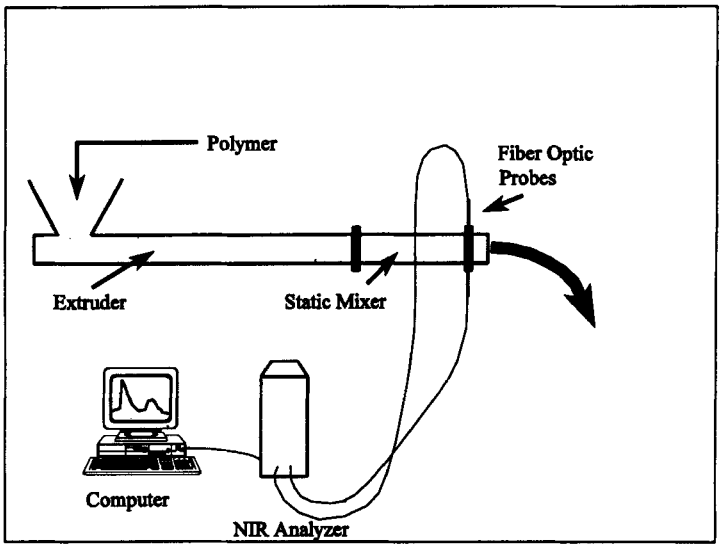

FIGURE 1: System used to obtain in-line NIR data.

arrangement of the equipment utilized. The NIR analyzer was equipped with 5.5 in. long optical probes with a sapphire lens with 0.25 in o.d. The probe body is manufactured out of 316 stainless steel. The transmission probes were inserted directly into the melt through a specially designed transition flange at the exit die. The probes were connected to the NIR analyzer using 2-m long single strand fiber optic cables protected by a PVC-coated aluminum monocoil jacket. In-line NIR scans of the blends were obtained using a pathlength of 5 mm. NIR scans were taken from 1100 to 2400 nm with a resolution of 2 nm. Eleven spectra resulted, one for each polymer blend composition examined. The analyzer was interfaced to a PC-compatible computer for control and data collection.

Fourier Transform Infrared Spectroscopy (FTIR): The polymer extrudate obtained from the pelletizer was used to make thin films for MIR analysis. Approximately 70 mg of polymer were weighed and placed between two sheets of aluminum foil in a constant thickness film maker (Specac, UK). The film makers consisted of two round metal platens with a spacer ring in which the polymer was heated and pressed. The whole assembly was placed into a hot press (Carver Inc., Wisconsin) operating at 180°C. The polymer sample was pre-heated for 5 min and pressed at 4 metric tons for 5 min. The film maker assembly was then placed into a cooling chamber for 5 minutes. Film thicknesses were approximately 250 μm. MIR spectra were obtained using a Mattson Galaxy GL-6020 FTIR spectrometer (Mattson Instruments, Madison, Wisconsin). A helium-neon laser was used as a light source with a mercury-cadmium-telluride detector. Samples were scanned 128 times with a resolution of 4 cm^{-1} from 400 to 4000 cm^{-1}. Single-sided interferograms were obtained with a mirror scanning velocity of 2.5 cm/s. The FTIR instrument was interfaced to a 486 PC-compatible computer for data acquisition.

RESULTS AND DISCUSSION

The results of applying PLS to convert NIR to MIR spectra can most easily be understood by considering a series of different types of graphical plots. These plots and their interpretation are as follows:

MIR and NIR Spectra

Figures 2 and 3 show the experimentally measured MIR and NIR spectra, respectively, for six of the polyethylene–polypropylene blends. In accordance with convention, the NIR spectra are plotted versus wavelength, whereas the MIR spectra are plotted versus wavenumber. Absorbance at various wavelengths in the MIR spectra can readily be assigned: strong methyl rocking vibrations from 841 to 972 cm^{-1}, CH_3 bending vibrations at 1377 and 1460 cm^{-1}, CH_2 rocking at 720 and 730 cm^{-1}, and so forth. However, from Barton et al. [7] we may anticipate that similar assignments for the NIR spectra are much more uncertain. Spectra for ten blends were used for the PLS calibration step. The spectra for the 50:50 blend was omitted from the calibration and used as the "unknown." In utilizing PLS, for MIR the wavelength range of 400 to 4000 cm^{-1} was regressed against the NIR range of 958 to 1237 cm^{-1}.

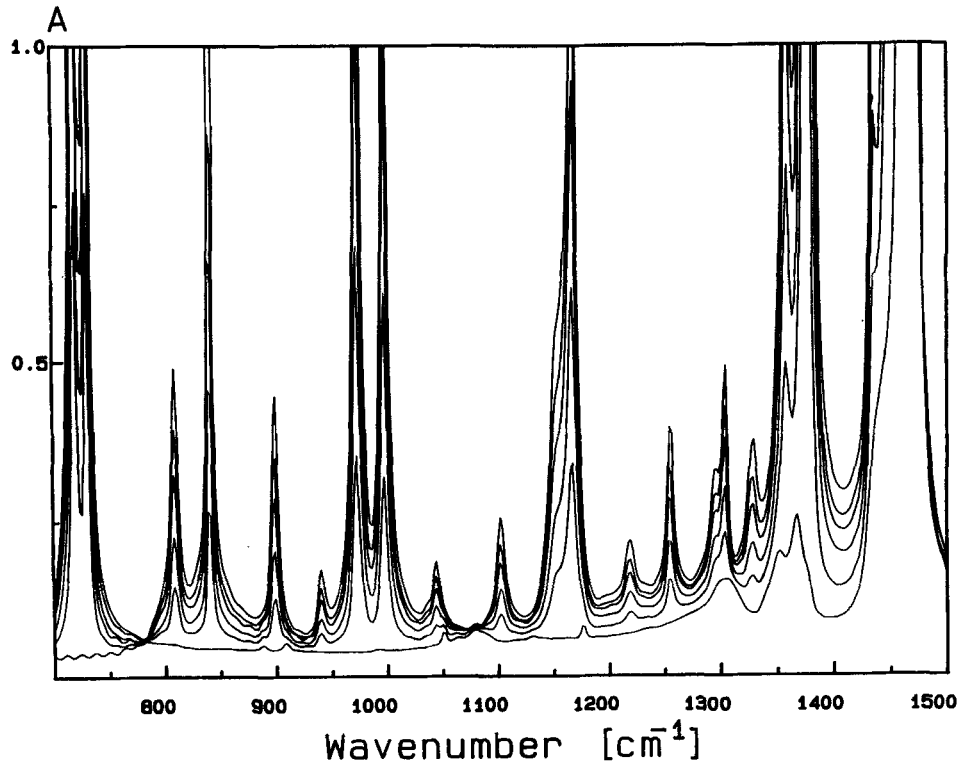

FIGURE 2: MIR calibration spectra obtained off-line (six of ten spectra shown) for polyethylene–polypropylene blends [8].

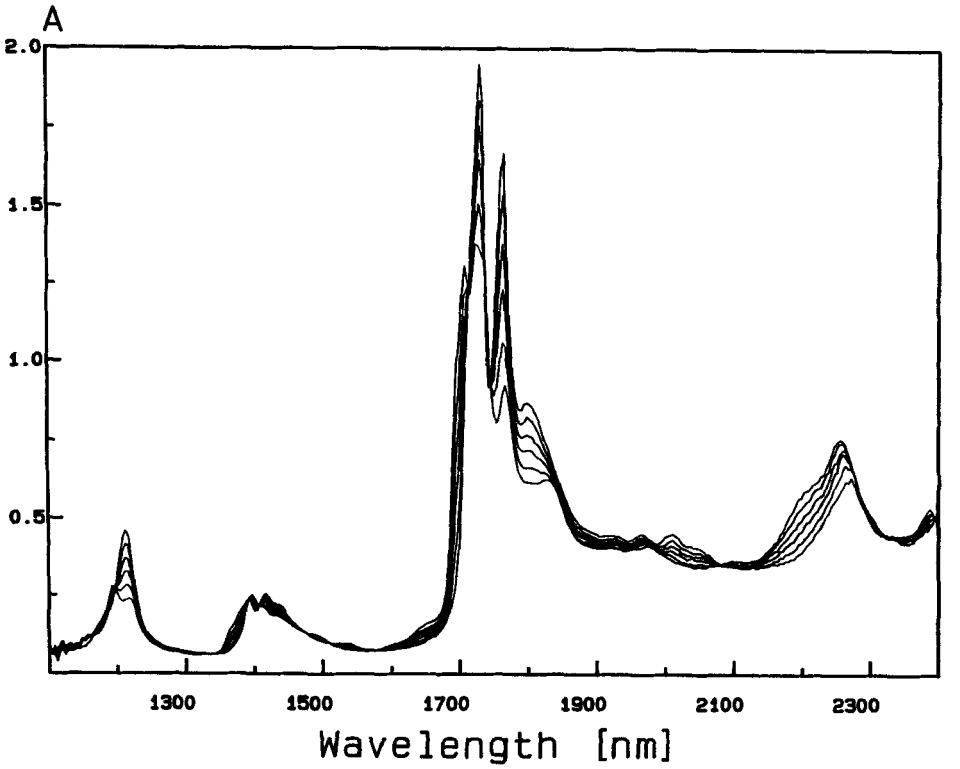

FIGURE 3: NIR calibration spectra obtained in-line (six of ten spectra shown) for polyethylene–polypropylene blends [8].

Standard Error of Prediction Plots

A plot of the SEP as a function of wavelength and number of factors enables the analyst to see when the SEP reaches a minimum as the number of factors is increased. By selecting only the first few (and most influential) factors, the important information is retained while noise is discarded. This also results in significant data compression. Figure 4 shows such a plot. From this figure it was evident that only one factor was necessary to predict the MIR spectrum in this region (958 to 1237 cm^{-1}): SEP shows only a very small additional decrease as the model progressively uses one to two factors, and beyond two factors the SEP actually begins to increase. The neighbouring two regions of the spectrum required three factors [8].

Loading Plots

A plot of P_{NIR} versus wavelength (a "factor loading plot") shows the NIR regions that are important for prediction of MIR spectra for a particular factor. Similarly, a plot of P_{MIR} versus wavelength shows the MIR regions where an important response will be seen for a particular factor.

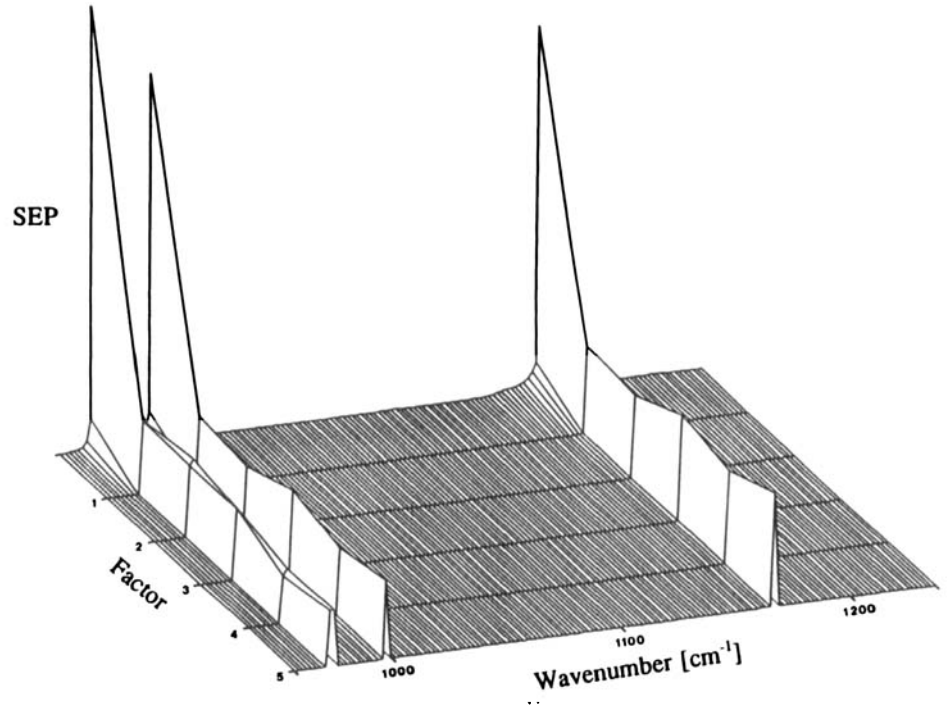

FIGURE 4: Standard error of prediction (a measure of how well the MIR spectrum for the 50:50 blend is predicted) versus the number of factors used [8].

Figures 5 and 6 show the plots of the loadings versus wavelength (P_{MIR} and P_{NIR}, respectively) for all regions examined when only one factor is used to explain the data for the "unknown." These plots resemble spectra and, when compared to Figures 2 and 3, revealed that practically all significant absorbances were contributing to the modelling.

Loading plots show the variables (in this case wavelength) that are most important to the model. Figure 7 is a plot of the PLS **second** factor loadings for the NIR spectra (as mentioned above, Figure 6 is for the **first** factor). This second factor plot illustrates the regions of the spectra where not all the variation of the data has been accounted. Regions where the variables show the most variation for a particular factor are indicated by high loadings. Figure 7 shows the regions where the variation in a particular variable were not completely accounted by the first factor. Regions that were accounted by the first factor are wavelength ranges where the loading is close to zero. The model used the remaining variation to try to improve the model prediction. Regions of high frequency fluctuation of the loading above and below zero indicate that noise is now being modeled and the data overfit. Hence, in addition to the use of the SEP plots, loading plots are a useful graphical method for the determination of the optimal number of factors required for the PLS model.

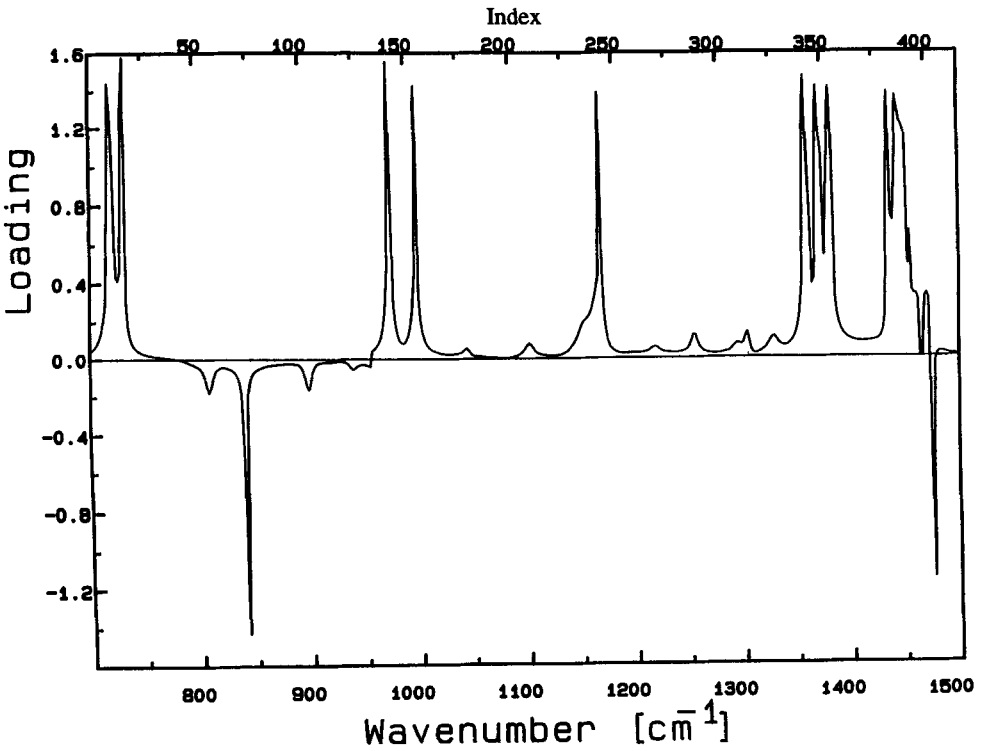

FIGURE 5: Loadings versus wavelength for MIR (P_{MIR}) for first factor [8].

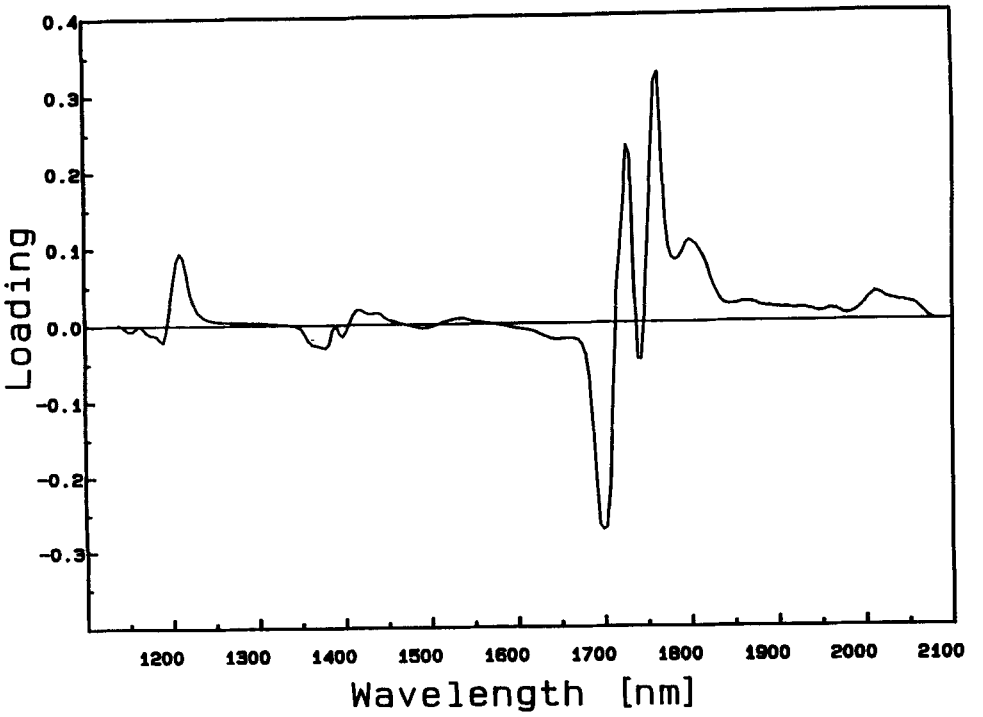

FIGURE 6: Loadings versus wavelength for NIR (P_{NIR}) for first factor.

Score Plots

Scores for a particular factor show the relationship of the individual samples to some underlying variation between samples. Figure 8 shows a plot of the scores for one and two factors versus sample number obtained from the PLS modelling for the first MIR wavelength region. Sample numbers were assigned from one to eleven in order of increasing polypropylene content. For the first factor, a good linear correlation was obtained between the samples. In this particular case, the variation can readily be attributed to the systematically different composition of the samples. The scores for the second factor are much lower in magnitude but indicate the presence of a possible second correlation amongst the samples. This correlation may be due to slight variations in the blend composition unaccounted for by the first factor or by some as yet undetermined regular varying property amongst them.

Predicted and Experimental MIR Spectra

Figure 9 shows the final result of the prediction of the MIR spectrum of the "unknown" from the NIR spectrum for all three regions of wavelength examined superimposed on the measured MIR spectrum. Agreement is excellent except for very strong absorbances that may well represent non-linear responses to concentration. Also, it appears that very narrow peaks with absorbance depending upon only one data point were more difficultto predict than broader peaks. The difference

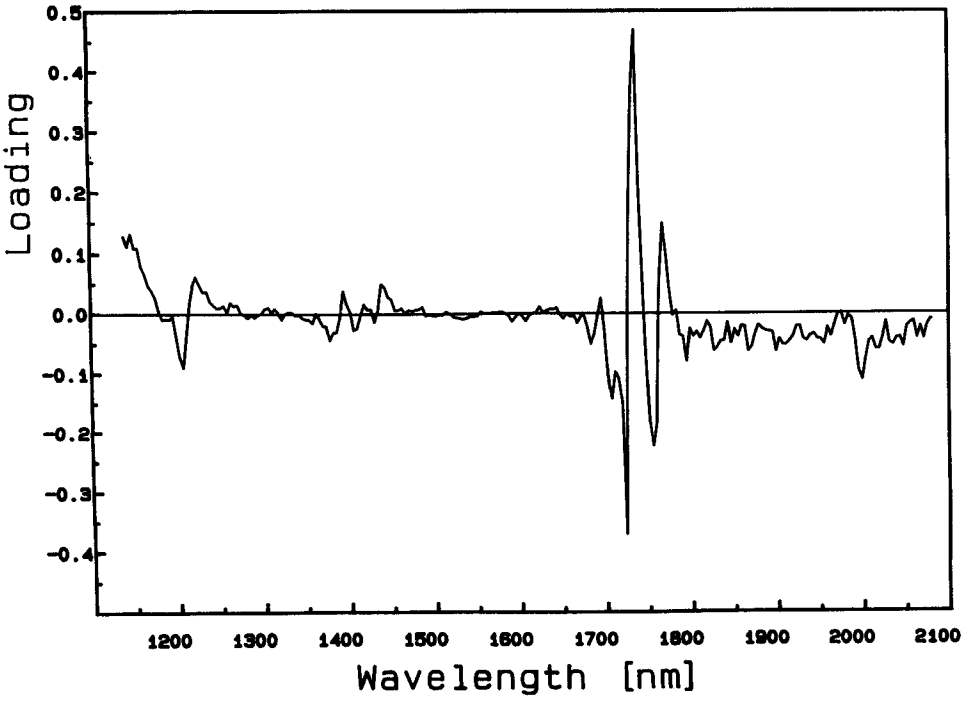

FIGURE 7: Loadings versus wavelength for NIR (P_{NIR}) for second factor.

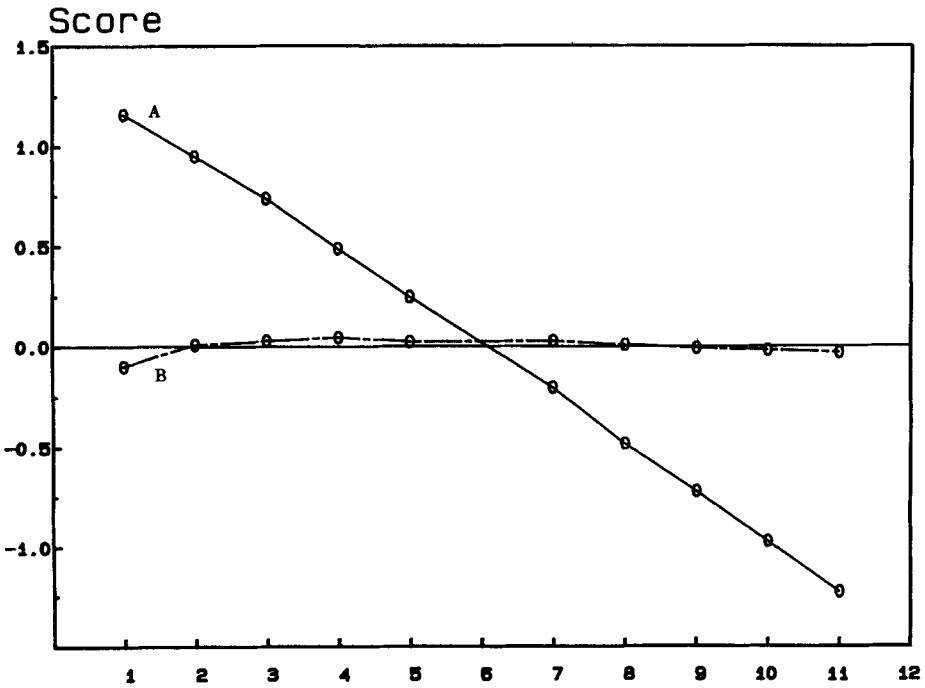

FIGURE 8: Scores versus sample number for: (A) one factor, (B) two factor.

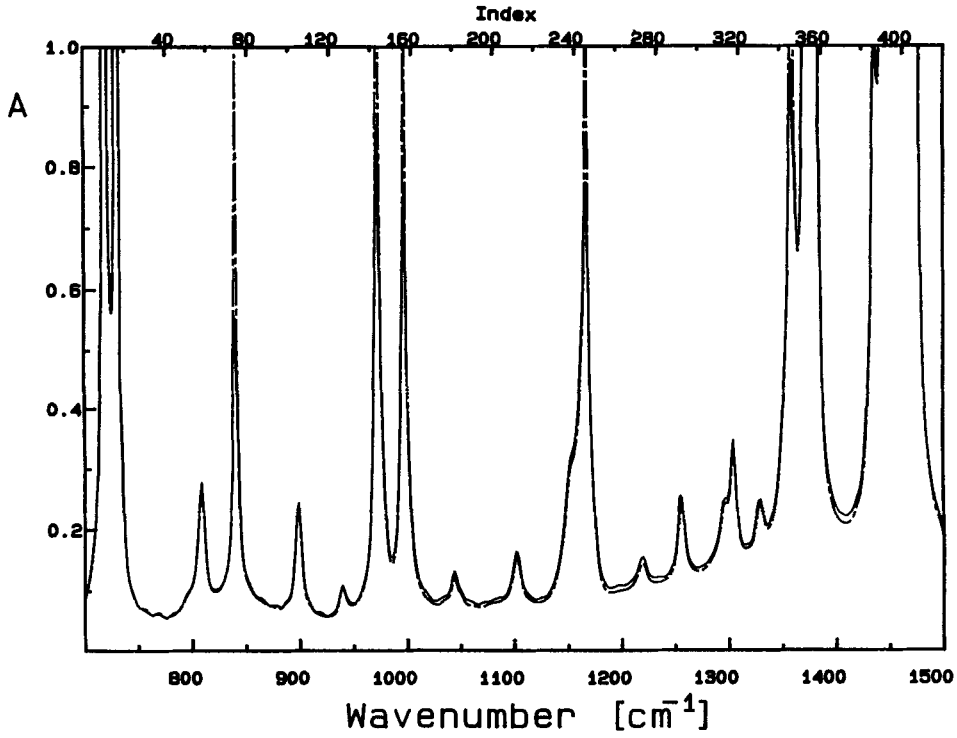

FIGURE 9: Measured (solid line) versus predicted (dashed line) for MIR spectrum of 50:50 blend [8].

between predicted and experimental MIR spectra can be examined closely using a plot of residuals (plotting the difference between the two spectra versus wavelength) [8].

The effect of an absorbing contaminant on the derived MIR spectrum has yet to be examined. However, detection of contaminants can be performed during both PLS calibration and prediction for a particular wavelength or sample. Hence, any peculiar NIR spectra or wavelength may be detected and removed from the model during calibration or during the prediction phase.

CONCLUSIONS

Partial least squares is an extremely powerful, but complex, numerical method that is greatly assisted by a variety of diagnostic plots. In a novel, unifying application of this method, when calibration spectra (i.e. corresponding NIR–MIR spectra) were supplied (but not concentrations), PLS readily predicted the MIR spectrum from the corresponding NIR spectrum. Agreement was excellent except for very strongly absorbing peaks. This provides the analyst with valuable and reassuring additional information, an entire MIR spectrum, to accompany the NIR spectrum.

Acknowledgments

We wish to thank the Ontario Centre for Materials Research and Eastman Kodak Company (Rochester, New York) for support of this research. We are also grateful to Dow Chemical Canada (Sarnia, Ontario) and Himont Canada Inc. (Montreal, Quebec) for providing materials.

References

1. P. Williams and K. Norris (eds.), *Near Infrared Technology in the Agricultural and Food Industries*, Amer. Assoc. of Cereal Chemists, Inc., St. Paul, Minnesota, 1990.
2. B. G. Osborne and T. Fearn, *Near Infrared Spectroscopy in Food Analysis*, J. Wiley and Sons, New York, 1986.
3. G. N. Foster, S. B. Snow, and R. G. Grisky, *J.l Appl. Polym. Sci.*, **8**, 1357 (1964).
4. E. W. Crandell, E. L. Johnson, and C. H. Smith, *J. Appl. Polym. Sci.*, **19**, 897 (1975).
5. I. E. W. Crandell and A. N. Jagtap, *J. Appl. Polym. Sci.*, **29**, 449 (1977).
6. C. E. Miller, *Appl. Spectrosc. Rev.*, **6**, 277 (1991).
7. F. E. Barton II, D. S. Himmelsbach, J. H. Duckworth, and M. J. Smith, *Appl. Spectrosc.*, **46**, 420 (1992).
8. R. Lew and S. T. Balke, *Appl. Spectrosc.*, **47**, 1747 (1993).
9. H. Martens and T. Naes, *Trends Anal. Chem.*, **3**(8), 204 (1984).
10. H. Martens and T. Naes, *Trends Anal. Chem.*, **3**(10), 266 (1984).
11. P. Geladi and B. R. Kowalski, *Anal. Chem.*, **59**, 1007A (1987).
12. K. R. Beebe and B. R. Kowalski, *Anal. Chim. Acta*, **185**, 1 (1986).
13. D. M. Haaland and E. V. Thomas, *Anal. Chem.*, **60**, 1193 (1988).
14. D. M. Haaland and E. V. Thomas, *Anal. Chem.*, **60**, 1202 (1988).
15. I. S. Helland, *Commun. Statist.-Simula.*, **17**, 581 (1988).
16. E. V. Thomas and D. M. Haaland, *Anal. Chem.*, **62**, 1091 (1990).
17. S. Clementi, C. Gabriele, C. Gianluca, *Anal. Chim. Acta*, **191**, 149 (1986).
18. D. M. Haaland, *Anal. Chem.*, **60**, 1208 (1988).
19. O. Matthias and G. Tutjiana, *Anal. Chim. Acta*, **200**, 379 (1987).
20. D. M. Haaland, R. G. Easterling and D. A. Vopicka, *Appl. Spectrosc.*, **39**, 73(1985).